

# An energy based approach for the control of a micro-robotic contact scenario <sup>★</sup>

Hector Ramirez Bilal Komati Yann Le Gorrec  
Cédric Clévy

*FEMTO-ST UMR CNRS 6174, AS2M department, University of  
Bourgogne Franche-Comté, University of Franche-Comté/ENSMM, 24  
rue Savary, F-25000 Besançon, France. (e-mail:  
{ramirez,legorrec}@femto-st.fr)*

---

**Abstract:** Energy based approaches have proven to be specially well suited for the modeling and control of mechanical systems. Among these approaches the port-Hamiltonian framework presents interesting properties for the structural modeling of complex systems and for the design of non-linear controllers using passivity. In this paper we use this framework to model a typical micro-robotic contact scenario and to propose a simple but effective globally stabilizing controller. The model and the controller take into account the transitions from a non-contact to a contact state (and the inverse) by the introduction of a non-linear (switching) contact element. A one degree of freedom experimental micro-robotic setup is used to test and illustrate the results.

*Keywords:* Passivity based control, port-Hamiltonian systems, non-linear control, micro-mechatronics

---

## 1. INTRODUCTION

At micro-scale there are several challenges that make the control particularly difficult to address: predominance of contact and surface forces over volume forces (such as weight), the lack of precise models, the dependency to environment conditions (temperature, humidity, light, etc), the parameter uncertainties, the difficulty of sensor integration and low signal to noise ratio. All these factors increase the complexity of modeling and control and may cause instabilities in the dynamic behavior of the system. In applications where contact interaction exists, such as in micro-assembly (Clévy et al., 2011) or mechanical ADN manipulation (Boudaoud et al., 2013), the problem of switching between contact and non-contact scenarios appears. These systems are frequently modeled as hybrid systems (Carloni et al., 2007). The switching between contact and non-contact scenarios can induce instability in closed-loop and proofs of global stability are often not considered. In such systems, controlling both the force and the position is often required, (Komati et al., 2013; Xu, 2015), which requires to integrate both force and position sensors into the micro-systems, a task not always simple at the considered scale.

In this paper the port-Hamiltonian framework is used to systematically model a typical micro-robotic contact scenario. The port-Hamiltonian system (PHS) handles the contact scenarios by introducing a switching variable in the dynamic model, similarly to the case of power-converters (Batlle et al., 2008; Ortega et al., 2001). The PHS is then instrumental to derive a passivity based controller

---

<sup>★</sup> This work was supported by French sponsored projects HAMEC-MOPSY and Labex ACTION under reference codes ANR-11-BS03-0002 and ANR-11-LABX-0001-01 respectively.

which accounts for the switching between contact and non-contact scenarios in the stability proof. The proposed controller can be derived and interpreted in the frame of Interconnection and Damping Assignment - Passivity Based Control (IDA-PBC) (Ortega et al., 2002). The control law is simple and only requires to measure position and velocity of the micro-robotic actuator. It is inherently robust since its a passivity based controller, which is an advantage in the case of micro-applications where parameters are often hard to estimate. An interesting feature of the approach is that the stability proof reduces to a polynomial equation, which could open perspectives in terms of robust analysis or approximated solutions. A typical 1-DOF micro-robotic experimental set-up is finally used to test and illustrate the control. The paper is organized as follows, Section 2 presents the contact scenario and the model in terms of a switching variable. Section 3 presents the port-Hamiltonian model. Section 4 the derivation of the passivity based controller and Section 5 the experimental results. Finally Section 6 gives some conclusion and comments on future work.

## 2. MODEL OF A 1-DOF CONTACT SCENARIO

The system under study is a micro-robot with an integrated sensorized end-effector. This micro-robot comes into contact with a flexible environment, considered as a compliant beam. The microrobot is modeled as a double mass-spring-damper (one for the actuation and other for sensing) and the flexible environment is modeled as a mass-spring-damper system. The concept is shown in Figure 1 and the model in Figure 2.

The study of contact scenario is especially important at the microscale where surface and contact forces can be

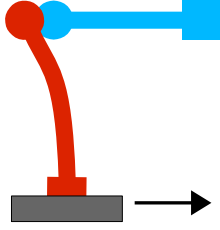


Fig. 1. Actuator (grey) end-effector (red), compliant beam (blue)

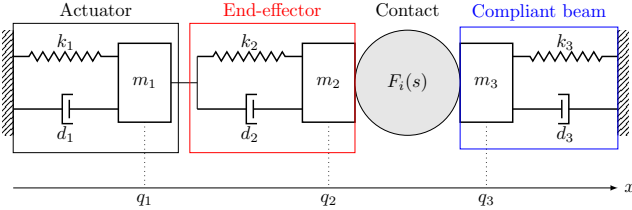


Fig. 2. The mechanical model including the contact element

come predominant. In the literature several models have been developed for microscale contact, most of them inspired from macroscale models, such as Johnson-Kendall-Roberts (JKR) Johnson (1987) and Derjaguin-Muller-Toporov (DMT) Derjaguin et al. (1975) models. However, these are quasi-static models and combine van der Waal, adhesion and electrostatic force models. Moreover, they consider specific cases, favorable geometries such as sphere/plane or cylinder/cylinder contacts, control of the quantity of liquid at the interface of two objects etc. These models lack the repeatably and are not able to exactly model the contact of more complex contact cases (such as plane/plane contact) due to the uncertainties and the parameter uncertainty.

In this paper we refer to a macroscale approach to model the contact extend it to the micro-robotic application under consideration. We shall use a regularized approach, also known as compliant formulation, which is assumes that the contact force can be formulated as a continuous function of the relative deformation between the compliant surfaces of the contact bodies Marhefka and Orin (1999). Within this framework, several models have been developed, and Hertz law's (Hertz, 1896) which accounts for a pure elastic force model remains the foundation for most contact models encountered in engineering applications. An alternative contact force approach that includes dissipative effects during the contact process is the Kelvin-Voigt model. This force model considers a linear spring in conjunction with a linear damper and can be expressed as (Khulief and Shabana, 1987):

$$F_i = k_i(q_3 - q_2) + d_i(\dot{q}_3 - \dot{q}_2)$$

where  $F_i$  denotes the contact (interaction) force,  $k_i$  the contact stiffness,  $b_i$  the contact damping coefficient and  $q_2$  and  $q_3$  refer to the relative displacements of subsystems 2 and 3, respectively, of Figure 2. Hunt and Crossley (Hunt and Crossley, 1975) showed that the linear spring-damper model does not represent the physical nature of energy transformations during the contact. Instead, they represented the contact force by the Hertz force-

deformation law with a nonlinear viscous-elastic element as:

$$F_i = k_i(q_3 - q_2)^n + \chi(q_3 - q_2)^n(\dot{q}_3 - \dot{q}_2) \quad (1)$$

where  $n$  is a constant between 1 and 2 and  $\chi$  is called the hysteresis damping factor. In general, the contact force can be represented by the sum of an elastic and a friction force

$$F_i = F_k + F_d$$

where  $F_k$  and  $F_d$  represents, respectively, the forces induced by elasticity and the friction. To take into account the contact scenario we introduce a switching variable.

*Definition 1.* The switching variable  $s$  is subject to the following rule:

$$s = \begin{cases} 1 & \text{if } q_2 \geq q_3 \\ 0 & \text{if } q_2 < q_3 \end{cases}$$

According to the previous definition the value  $s = 0$  indicates that a contact exists wherever  $s = 1$  that it doesn't. Notice that the switch is treated as a discrete input to the system. This is the most simple manner to take into account the contact between the end-effector and the compliant beam since it follows a simple logical rule. Using the switching variable to define (2) we have

$$F_i(s) = sF_k + sF_d. \quad (2)$$

We shall make the following assumptions on the nature of the elastic and dissipative forces.

*Assumption 2.* The energy stored in the contact element is characterized by  $F_k$  and satisfies

$$W = s \int F_i(z) dz \geq 0. \quad (3)$$

The dissipative force is proportional to the velocity difference of the elements in contact

$$F_d(s) = d_i(q_2, q_3, s)(\dot{q}_3 - \dot{q}_2), \text{ with } d_i(s) = sd_i \quad (4)$$

The energy stored in the contact spring is positive (or zero if no deformation) since it corresponds to the physical energy stored by the elastic deformation effect.

### 3. A PORT-HAMILTONIAN DESCRIPTION

Consider the model of the actuator in Figure 2, it corresponds to a mass-spring-damper system described by the dynamic equations

$$\begin{aligned} \dot{q}_1 &= \frac{p_1}{m_1} \\ \dot{p}_1 &= -k_1 q_1 - b_1 \frac{p_1}{m_1} + F_s \end{aligned} \quad (5)$$

where  $q_1$  is the relative position,  $p_i$  the momentum of the mass and where  $F_s$  represents the force applied by the end-effector on the actuator. The dynamic model (5) is derived from the generalized Kirchhoff's relations (Newton's law) together with the formalization of the constitutive relations of each component, characterized by the definition of the energy of the conservative components (mass and spring) and the dissipated power of the resistive elements (damper). It is possible to write (5) as a linear relation between flows ( $\dot{q}_1, \dot{p}_1$ ) and efforts ( $k_1 q_1, \frac{p_1}{m_1}$ )

$$\begin{bmatrix} \dot{q}_1 \\ \dot{p}_1 \end{bmatrix} = \begin{bmatrix} 0 & 1 \\ -1 & -d_1 \end{bmatrix} \begin{bmatrix} k_1 q_1 \\ \frac{p_1}{m_1} \end{bmatrix} + \begin{bmatrix} 0 \\ 1 \end{bmatrix} F_s$$

by formalizing Kirchhoff's relations by a power preserving geometric structure. Define  $J = -J^T = \begin{bmatrix} 0 & 1 \\ -1 & 0 \end{bmatrix}$ ,  $R =$

$R^T = \begin{bmatrix} 0 & 0 \\ 0 & d_0 \end{bmatrix} \geq 0$  and  $g = \begin{bmatrix} 0 \\ 1 \end{bmatrix}$ , which represent respectively, the topology (geometric structure), the dissipation and the input map of the system. A port-Hamiltonian representation (Maschke and van der Schaft, 1992) of (5) is then given by

$$\begin{aligned} \dot{x}_1 &= (J - R) \frac{\partial H_1}{\partial x_1} + g F_s \\ y &= g^\top \frac{\partial H_1}{\partial x'} \\ \dot{H}_1 &= - \frac{\partial H_1}{\partial x_1}^\top R \frac{\partial H_1}{\partial x_1} + y_1^\top u_1 \end{aligned} \quad (6)$$

where  $x_1 = [q_1, p_1]$  is the state vector,  $H_1 = \frac{1}{2}k_1q_1^2 + \frac{1}{2m_1}p_1^2$  the Hamiltonian function. and  $y_1 = \frac{p_1}{m_1}$  is the output, which is conjugated to the input  $u_1 = F_s$ . The time variation of energy depends only on the presence of energy dissipating elements and the exchange with the environment through the input and output. Hence, by construction, if the Hamiltonian is bounded from below as in the case of a mechanical system, a PHS is passive and thus a stable system (Willems, 1972). This property is very important for modeling of complex systems and for the synthesis of Lyapunov based non-linear controllers (van der Schaft, 2000).

One of the features of PHS is that since they are defined with respect to power conjugated inputs and outputs, the power preserving interconnection of PHS renders the interconnected system PHS. Let us use this feature on the complete system described in Figure 2. The total energy is given by

$$\begin{aligned} H &= \frac{k_1}{2}q_1^2 + \frac{k_2}{2}(q_2 - q_1)^2 + \frac{k_3}{2}q_3^2 + W(q_2, q_3, s) \\ &\quad + \frac{p_1^2}{2m_1} + \frac{p_2^2}{2m_2} + \frac{p_3^2}{2m_3}. \end{aligned} \quad (7)$$

where  $q_i$  and  $p_i$ ,  $i = 1, 2, 3$ , represents the relative positions and momentum of each subsystem. The port-Hamiltonian model of the total system can then be deduced by interconnecting the subsystems through their conjugated inputs and outputs (van der Schaft, 2000). Taking as state vector  $x = [q_1, q_2, q_3, p_1, p_2, p_3]$  we obtain the following representation

$$\begin{pmatrix} \dot{q}_1 \\ \dot{q}_2 \\ \dot{q}_3 \\ \dot{p}_1 \\ \dot{p}_2 \\ \dot{p}_3 \end{pmatrix} = (J - R) \begin{pmatrix} k_1q_1 - k_2(q_2 - q_1) \\ k_2(q_2 - q_1) + \frac{\partial W}{\partial q_2}(s) \\ k_3q_3 + \frac{\partial W}{\partial q_3}(s) \\ \frac{p_1}{m_1} \\ \frac{p_2}{m_2} \\ \frac{p_3}{m_3} \end{pmatrix} + \begin{pmatrix} 0 \\ 0 \\ 0 \\ 1 \\ 0 \\ 0 \end{pmatrix} u \quad (8)$$

with  $J = \begin{pmatrix} 0 & I \\ -I & 0 \end{pmatrix}$ ,  $R = \begin{pmatrix} 0 & 0 \\ 0 & D(s) \end{pmatrix}$  with

$$D = \begin{pmatrix} d_1 + d_2 & -d_2 & 0 \\ -d_2 & d_2 + d_i(s) & -d_i(s) \\ 0 & -d_i(s) & d_3 + d_i(s) \end{pmatrix} \quad (9)$$

and conjugated output  $y = \frac{p_1}{m_1}$ . The dynamic contribution of the contact element appears in the gradient of the Hamiltonian (as an effort) and as a (non-linear) damping

coefficient in the dissipation matrix  $R$ . This is consistent with the physical interpretation: at the moment of a contact some energy is stored due to the elastic property of the deformation of the materials, and some energy is irreversible dissipated due to irreversible thermodynamic transformation of the matter. Notice that the matrix  $D(s)$  depends on the switching variable, but no matter which switching position it always remains positive definite, i.e.,  $D(s) > 0$ , for  $s = 0$  and  $s = 1$ . The time derivative of the total energy is given by

$$\begin{aligned} \dot{H} &= - \frac{\partial H}{\partial x}^\top R \frac{\partial H}{\partial x} + y^\top u \\ \dot{H} &= - \begin{bmatrix} p_1 & p_2 & p_3 \\ m_1 & m_2 & m_3 \end{bmatrix} D(s) \begin{bmatrix} p_1 \\ p_2 \\ p_3 \\ m_3 \end{bmatrix} + y^\top u \end{aligned}$$

This implies: i) that the system is dissipative with minimum at  $H(0) = 0$ , and ii) that the system cannot generate instantaneous energy due to the switching (contact). Indeed, it follows from the previous derivative that the energy is at all moment bounded by the initial energy in the system. The first remark is just a consequence of the PH structure. The second remark is important since it implies that the system remains PH (and hence passive) for any switching sequence. This is similar to the case of power-converters (Ortega et al., 2001; Batlle et al., 2008), with the difference that in our case the switching explicitly appears in the energy balance.

#### 4. STABILIZATION BY PASSIVITY BASED CONTROL

The control objective is to control the gripping force which at equilibrium is proportional to the  $q_3$  coordinate,  $F_3^* = k_3q_3^*$ , where  $(\cdot)^*$  demotes equilibrium configurations. To stabilize an arbitrary equilibrium  $x^*$ , we may proceed to shape the closed-loop Hamiltonian function or to change the complete structure of the closed-loop system such that is Lyapunov stable with respect to a shaped closed-loop Hamiltonian. A classical technique in passivity based control for PHS is the celebrated energy shaping control by the Casimir method (Ortega et al., 2001). This method consists in finding the geometric invariants of the closed-system, considering the controller as a PH control system. This permits to compute a control that renders the closed-loop system a PHS with respect to a shaped Hamiltonian function. For our case it is straightforward to verify that using the Casimir method we are only able to shape the closed-loop Hamiltonian in the  $q_1$  coordinate, which is not enough since the desired closed-loop equilibrium is of the form  $x^* = [q_1^*, q_2^*, q_3^*, 0, 0, 0]$ , i.e., it is required to shape the Hamiltonian in all the  $q$  coordinates.

*Proposition 3.* If the matching equation

$$\begin{aligned} W_d &= W(s) + f(q_1) + k_{2a}q_1q_2 - k_{2a}q_2^2 \\ &\quad - k_{2d}(q_1^* - q_2^*)q_2 + k_{3a}q_3^*q_3 - k_{3a}q_3^2 + c \end{aligned} \quad (10)$$

subject to

$$W_d \geq 0, \quad W_d = 0 \text{ if } x = x^* \quad (11)$$

is satisfied, with  $W_d(s) = sW_d$  a desired closed-loop contact function,  $k_{i_a} = k_i + k_{i_a}$ ,  $i = 1, 2, 3$  desired stiffness coefficients,  $f(q_1)$  an arbitrary function of  $q_1$  and  $c$  a constant, then the control  $u = \beta(x, x^*)$ , with

$$\beta = k_1 q_1^* - k_{1_a}(q_1 - q_1^*) + k_2(q_1^* - q_2^*) + k_{2_a}((q_2 - q_2^*) - (q_1 - q_1^*)) - \frac{\partial W_d}{\partial q_1} \quad (12)$$

asymptotically stabilizes the closed-loop system at  $x = x^*$

**Proof.** Consider the following closed-loop Hamiltonian function

$$H_d = \frac{k_{1_d}}{2}(q_1 - q_1^*)^2 + \frac{k_{2_d}}{2}((q_2 - q_2^*) - (q_1 - q_1^*))^2 + \frac{k_{3_d}}{2}(q_3 - q_3^*)^2 + W_d(q_1, q_2, q_3, q_1^*, q_2^*, q_3^*, s) + \frac{p_1^2}{2m_1} + \frac{p_2^2}{2m_2} + \frac{p_3^2}{2m_3}$$

Taking the time derivative of  $H_d$  along the trajectories of (8) gives

$$\begin{aligned} \dot{H}_d &= \frac{p_1}{m_1}(-k_1 q_1^* + k_{1_a}(q_1 - q_1^*) - k_2(q_1^* - q_2^*)) \\ &+ \frac{p_1}{m_1}(-k_{2_a}((q_2 - q_2^*) - (q_1 - q_1^*)) + \frac{\partial W_d}{\partial q_1} + u) \\ &+ \frac{p_2}{m_2}(k_2(q_1^* - q_2^*) + k_{2_a}((q_2 - q_2^*) - (q_1 - q_1^*))) \\ &+ \frac{p_2}{m_2}\left(-\frac{\partial W}{\partial q_2}(s) + \frac{\partial W_d}{\partial q_2}\right) \\ &+ \frac{p_3}{m_3}\left(-k_3 q_3^* + k_{3_a}(q_3 - q_3^*) - \frac{\partial W}{\partial q_3}(s) + \frac{\partial W_d}{\partial q_3}\right) \\ &- d_1\left(\frac{p_1}{m_1}\right)^2 - d_2\left(\frac{p_1}{m_1} - \frac{p_2}{m_2}\right)^2 - d_i(s)\left(\frac{p_2}{m_2} - \frac{p_3}{m_3}\right)^2 \\ &- d_3\left(\frac{p_3}{m_3}\right)^2 \end{aligned} \quad (13)$$

We observe from (13) that  $H_d \leq 0$  and  $H_d = 0$  only at  $x = x^*$  if the following conditions are satisfied

$$-k_1 q_1^* + k_{1_a}(q_1 - q_1^*) - k_2(q_1^* - q_2^*) - k_{2_a}((q_2 - q_2^*) - (q_1 - q_1^*)) + \frac{\partial W_d}{\partial q_1} + u = 0 \quad (14)$$

$$k_2(q_1^* - q_2^*) + k_{2_a}((q_2 - q_2^*) - (q_1 - q_1^*)) - \frac{\partial W}{\partial q_2}(s) + \frac{\partial W_d}{\partial q_2} = 0 \quad (15)$$

$$-k_3 q_3^* + k_{3_a}(q_3 - q_3^*) - \frac{\partial W}{\partial q_3} + \frac{\partial W_d}{\partial q_3}(s) = 0 \quad (16)$$

together with the conditions on  $W_d$  given in (11). Condition (14) gives the control (12), while conditions (15) and (16) correspond to matching conditions (Ortega et al., 2002) of the control design problem. Integrating (15) and (16) we obtain (10). Finally, by applying LaSalle's invariance principle on region around  $x^*$  we conclude that  $\beta(x, x^*)$  asymptotically stabilizes the closed-loop system at  $x = x^*$ .

Equation (10) is a polynomial equation if the model of contact element and  $f(q_1)$  are polynomial functions, with  $f(q_1)$ ,  $k_{2_a}$ ,  $k_{3_a}$  and  $c$  to be determined such that  $W_d$  satisfies (11). Notice that we are imposing  $W_d = 0$  at  $x = x^*$ , but we are not imposing any condition on  $W_d$  when there is no contact. Since  $W_d$  is the desired contact energy function it is a degree of freedom in the control design to impose or not  $W_d = 0$  when  $s = 0$ . The contribution to the control action of  $W_d$  is only through the term  $\frac{\partial W_d}{\partial q_1}$ . Hence, if  $W_d = W_d(q_1, q_2)$  the control action is independent of the model of the contact element.

From (13) we observe that any dissipative term of the form  $d_d(x)\frac{p_1}{m_1}$ , with  $d_d(x) > 0$  a positive function of  $x$ , adds additional dissipation to the closed-loop system without changing the matching equation (10). Hence the most

general control which asymptotically stabilizes the closed-loop system with respect to the closed-loop Hamiltonian  $H_d$  is

$$u = \beta(x, x^*) - d_d(x)\frac{p_1}{m_1}. \quad (17)$$

The proposed control can be interpreted in terms of (parametrized) Interconnection and Damping Assignment - Passivity Based Control (IDA-PBC) (Ortega et al., 2001, 2002). Indeed, the matching condition (10) and the control (17) render the closed-loop system in PHS format

$$\dot{x} = (J - R_d)\frac{\partial H_d}{\partial x} \quad (18)$$

with closed-loop energy balance

$$\dot{H}_d = -\frac{\partial H_d}{\partial x}^\top R_d \frac{\partial H_d}{\partial x}$$

where  $R_d = \begin{pmatrix} 0 & 0 \\ 0 & D(s) + D_d \end{pmatrix}$  with

$$D_d = \begin{pmatrix} d_d(x) & 0 & 0 \\ 0 & 0 & 0 \\ 0 & 0 & 0 \end{pmatrix} \quad (19)$$

Its important to remark that the matching equations (15)-(16) reduce to one algebraic polynomial equation. This is an important relaxation since the cornerstone in IDA-PBC design methods are the matching conditions which generally correspond to semi-linear partial differential equations (PDEs). For the class of system under study, considering polynomial contact elements, the matching conditions is a polynomial equation.

Notice that until now no assumption has been made on the form of  $W$  except for that  $W \geq 0$  and  $W = 0$  if the systems are not in contact, i.e.,  $s = 1$ . In the following subsection we shall compute the control (17) for a specific choice of contact element.

#### 4.1 PBC for a class of contact elements

In this subsection we will consider a simple model of the contact, in order to compute the solutions analytically. A classical contact spring-dashpot Gilardi and Sharf (2002) model shall be used to characterize the contact

$$F_i = sk_i(q_3 - q_2) + sd_i\left(\frac{p_3}{m_3} - \frac{p_2}{m_2}\right)$$

with  $k_i$  and  $d_i$  positive constants. The energy of the contact spring is then simply given by

$$W = \frac{1}{2}k_i s(q_3 - q_2)^2 \quad (20)$$

Let us consider the matching condition (10) for this model.

$$W_d = \frac{1}{2}k_i s(q_3 - q_2)^2 + f(q_1) + k_{2_a}(q_1 - (q_1^* - q_2^*))q_2 - k_{2_a}q_2^2 - k_2(q_1^* - q_2^*)q_2 + k_{3_d}q_3^*q_3 - k_{3_a}q_3^2 + c.$$

To simplify the previous equation we chose  $f(q_1) = k_{2_a} = k_{3_a} = 0$  to obtain

$$W_d = \frac{1}{2}k_i s(q_3 - q_2)^2 - k_2(q_1^* - q_2^*)q_2 + k_{3_d}q_3^*q_3 + c. \quad (21)$$

From the equilibrium conditions of the dynamical system (8) we have that

$$\begin{aligned} sk_i(q_3^* - q_2^*) + k_{3_d}q_3^* &= 0, \\ sk_i(q_3^* - q_2^*) + k_2(q_1^* - q_2^*) &= 0. \end{aligned}$$

Using these relations in (21) and completing squares we obtain

$$W_d = \frac{1}{2} k_i s ((q_3 - q_3^*) - (q_2 - q_2^*))^2$$

with  $c = (q_3^* - q_2^*)^2$ . The control law is derived from (17) and is for this case

$$u = k_1 q_1^* - k_{1_a} (q_1 - q_1^*) + k_2 (q_1^* - q_2^*) - d_d(x) \frac{p_1}{m_1}, \quad (22)$$

and renders the closed-loop system a PHS as in (18) with respect to the closed-loop energy function

$$\begin{aligned} H_d = & \frac{k_{1_d}}{2} (q_1 - q_1^*)^2 + \frac{k_2}{2} ((q_2 - q_2^*) - (q_1 - q_1^*))^2 \\ & + \frac{k_3}{2} (q_3 - q_3^*)^2 + \frac{1}{2} k_i s ((q_3 - q_3^*) - (q_2 - q_2^*))^2 \\ & + \frac{p_1^2}{2m_1} + \frac{p_2^2}{2m_2} + \frac{p_3^2}{2m_3} \end{aligned}$$

The control tuning parameters (see (22)) are the added stiffness  $k_{1_a} > 0$  in the first spring ( $q_1$  coordinate) and the added dissipation function  $d_d(x) > 0$  which acts on the  $p_1$  coordinate. Notice that the control action does not depend on the contact element since  $W = W(q_2, q_3)$ .

*Remark 4.* A very simple contact model has been used to compute an exact solution for (10). However, since (10) is of polynomial nature we can expect to use polynomial fitting algorithms to compute approximated solutions of  $W_d$  and evaluate the robustness of the approximated solutions in terms of LMIs for instance. This is the subject of study of ongoing work.

## 5. EXPERIMENTAL RESULTS

To test the robustness of the controller the set-up of Figure 3 was implemented in a laboratory environment. We refer the reader to Komati et al. (2013) for a detailed description of the set-up. A glass micro-structure with  $300\mu\text{m}$  of thickness was used as the passive compliant environment and it was attached to a fixed base. A Femto-Tools force sensing probe FT-S270 attached to a positioning stage, with a sensing range of  $2\text{mN}$ , was used as end-effector. The end-effector comprises a probe of  $3\text{mm}$  of length and  $50\mu\text{m}$  of thickness, that moves along the  $X$  direction according to Figure 3. The displacement is measured with a capacitive sensor. The maximal contact surface between the end-effector and the environment is  $50\mu\text{m} \times 50\mu\text{m}$ . The positioning stage is a PXY D12 - piezo XY scan positioner from PiezoSystemJena with a travel range of  $200\mu\text{m}$ . It has an internal capacitive sensor to measure the displacement of the stage along its two axis. A Keyence laser sensor is used to measure the displacement of the compliant beam. The positioning stage was controlled and the force and the position feedback were acquired through a dSPACE1104 board.

The parameters of the experimental set-up were identified following the procedure of Komati et al. (2013) and are summarized in Table 1. The comparison between the open-loop step-response is shown in Figure 4. The input was chosen such that the system experienced non-contact/contact transitions. The positions  $q_1$  and  $q_3$  and the force  $F_3 = k_3 q_3$  are measured in experiments and compared to the simulation model. The experimental set-up presents more oscillations compared to the simulations

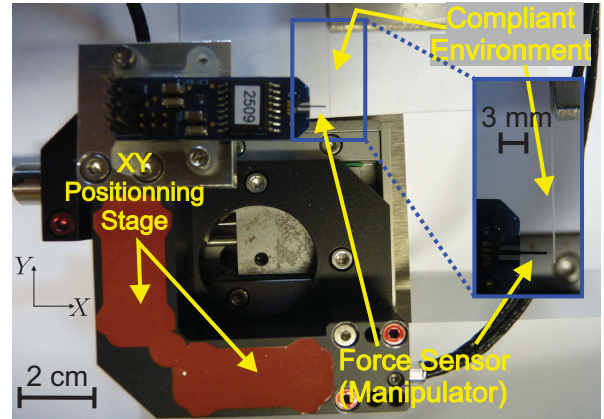


Fig. 3. Experimental setup of the contact scenario

Parameter	Value
$k_1$	1.01
$d_1$	0.013
$m_1$	$6.27 \times 10^{-5}$
$k_2$	1170
$d_2$	0.001
$m_2$	$1.05 \times 10^{-7}$
$k_3$	47
$d_3$	0.001
$m_3$	$1 \times 10^{-6}$
$k_i$	327.5
$d_i$	$1 \times 10^{-4}$
$L_2$	$8 \mu\text{m}$
$L_3$	$20 \mu\text{m}$

Table 1. Parameters of the micro-process

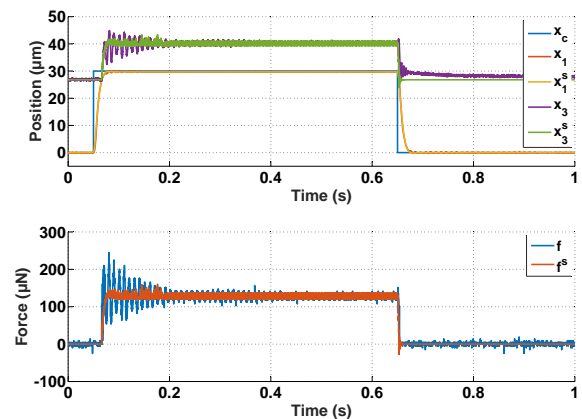


Fig. 4. Open-loop step-responses of  $q_1$ ,  $q_3$  and  $F_3$ . Super-index  $s$  denotes simulations

and this difference is mostly produced by the damping element in the contact-element of the model.

For the control the reference of the system is the value  $q_3^*$  which is calculated to achieve a desired force  $F_3^*$ . The force reference is calculated using the static relation  $F_3^* = k_3 q_3^*$ . Figure 5 shows the closed-loop response. A reference  $q_3^*$  is applied to the system at  $t = 0.05\text{s}$ , then the robot's end-effector starts to move towards contact until  $t = 0.06\text{s}$  where  $q_2$  becomes greater or equal to  $q_3$  which switches the closed-loop model to the contact case. A force

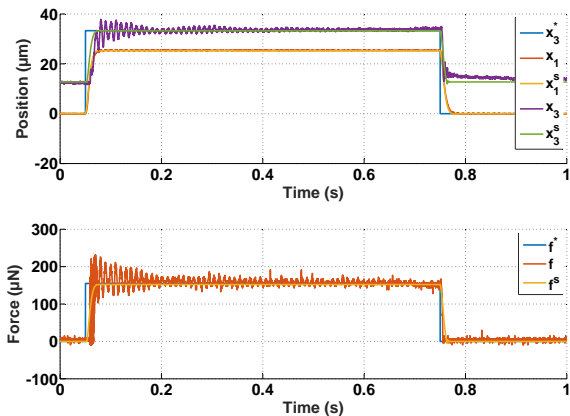


Fig. 5. Closed-loop step-responses of  $q_1$ ,  $q_3$  and  $F_3$ . Super-index  $s$  denotes simulations

appears due to the contact and the force oscillates for around 400ms around the reference force. The experiment shows that even though a very simple switching rule was chosen closed-loop model accounts for the the contact phenomenon. The control was implemented as in (22), i.e., without using the measures of  $q_3$  and  $F_3$ . Nevertheless, provided that the stiffness of the compliant beam is sufficiently well estimated the controller manages to follow the desired force reference with small error. Its interesting to mention that a very simple solution for the contact model has been used in the derivation of the control law. The closed-loop system remains stable since passivity based controllers are inherently robust. However, a measure of robustness is desired, particularly for micro-robotic applications where parameter uncertainties are high. This is the subject of ongoing work.

## 6. CONCLUSION

The port-Hamiltonian framework has been used to systematically model a typical micro-robotic contact scenario. The PHS handles the contact scenarios by introducing a switching variable in the dynamic model, similarly to the case of power-converters. The PHS has been instrumental to derive a globally stabilizing passivity based controller which accounts for the switching between contact and non-contact. The proposed controller can be derived and interpreted in the frame of IDA-PBC. Within that frame, the matching condition of this control problem is given as a polynomial equation, which is an interesting feature since it could be studied using tools from convex analysis. The control law is simple and only requires to measure position and velocity of the micro-robotic actuator. An 1-DOF micro-robotic experimental set-up was used to test the controller. Ongoing work is studying the robustness of the controller and the addition of adaptive control action.

## REFERENCES

Battle, C., Dria-Cerezo, A., and Fossas, E. (2008). Bidirectional power flow control of a power converter using passive hamiltonian techniques. *International Journal of Circuit Theory and Applications*, 36(7), 769–788.

- Boudaoud, M., Haddab, Y., Le Gorrec, Y., and Lutz, P. (2013). Modeling and optimal force control of a nonlinear electrostatic microgripper. *IEEE/ASME Transactions on mechatronics*, 18, 1130 – 1139.
- Carloni, R., Sanfelice, R., Teel, A., and Melchiorri, C. (2007). A hybrid control strategy for robust contact detection and force regulation. *American Control Conference*, 1461–1466.
- Clévy, C., Rakotondrabe, M., and Chaillet, N. (2011). *Signal Measurement and Estimation Techniques for Micro and Nanotechnology*. Springer.
- Derjaguin, B., Muller, V., and Toporov, Y. (1975). Effect of contact deformations on the adhesion of particles. *Journal of Colloid and Interface Science*, 53, 314326.
- Gilardi, G. and Sharf, I. (2002). Literature survey of contact dynamics modelling. *Mechanism and Machine Theory*, 37, 12131239.
- Hertz, H. (1896). On the contact of solids - on the contact of rigid elastic solids and on hardness. In: *Miscellaneous Papers (Translated by D.E. Jones and G.A. Schott)*, Macmillan and Co., 146183.
- Hunt, K. and Crossley, F. (1975). Coefficient of restitution interpreted as damping in vibroimpact. *Journal of applied mechanics*, 7, 440–445.
- Johnson, K. (1987). *Contact mechanics*. Cambridge University Press.
- Khulief, Y. and Shabana, A. (1987). A continuous force model for the impact analysis of flexible multibody systems. *Mech. Mach. Theory*, 22, 213–224.
- Komati, B., Rabenoroso, K., Clévy, C., and Lutz, P. (2013). Automated guiding task of a flexible micropart using a two-sensing-finger microgripper. *IEEE Transactions on Automation, Science and Engineering*, 10(3), 515–524. doi:10.1109/TASE.2013.2241761.
- Marhefka, D. and Orin, D. (1999). A compliant contact model with nonlinear damping for simulation of robotic systems. *IEEE Transactions on Systems, Man and Cybernetics - Part A: Systems and Humans*, 29, 566572.
- Maschke, B. and van der Schaft, A.J. (1992). Port-controlled Hamiltonian systems: modelling origins and systemtheoretic properties. *Proceedings of the International Symposium on Nonlinear Control Systems Design, NOLCOS'92, Bordeaux, France, June*.
- Ortega, R., van der Schaft, A., Maschke, B., and Escobar, G. (2002). Interconnection and damping assignment passivity based control of port-controlled Hamiltonian systems. *Automatica*, 38, 585–596.
- Ortega, R., van der Schaft, A.J., Mareels, I., and Maschke, B. (2001). Putting energy back in control. *Control Systems Magazine*, 21, 18–33.
- van der Schaft, A.J. (2000). *L2-Gain and Passivity Techniques in Nonlinear Control*.
- Willems, J. (1972). Dissipative dynamical systems part I: General theory. *Archive for Rational Mechanics and Analysis*, 45, 321–351.
- Xu, Q. (2015). Robust impedance control of a compliant microgripper for high-speed position/force regulation. *IEEE Transactions on Industrial Electronics*, 62(2), 1201–1209. doi:10.1109/TIE.2014.2352605.